Enhanced Oral Bioavailability of 2′-β-fluoro-2′,3′-dideoxyadenosine (F-ddA) through Local Inhibition of Intestinal Adenosine Deaminase

R. Tyler DeGraw[1] and Bradley D. Anderson[1,2]

Received March 21, 2001; accepted June 6, 2001

Purpose. Intestinal enzyme inhibition may be an effective tool to increase the oral bioavailability of compounds that undergo first-pass intestinal metabolism. However, systemic enzyme inhibition may be undesirable and therefore should be minimized. 2-β-fluoro-2′,3′-dideoxyadenosine (F-ddA) is an adenosine deaminase (ADA) activated prodrug of 2-β-fluoro-2′,3′-dideoxyinosine (F-ddI) with enhanced delivery to the central nervous system (CNS) that has been tested clinically for the treatment of AIDS. Unfortunately, intestinally localized ADA constitutes a formidable enzymatic barrier to the oral absorption of F-ddA. This study explores various factors involved in inhibitor selection and dosage regimen design to achieve local ADA inhibition with minimal systemic inhibition.

Methods. *In situ* intestinal perfusions with mesenteric vein cannulation were performed in the rat ileum to determine the lumenal disappearance and venous blood appearance of F-ddA and F-ddI. Coperfusions with the ADA inhibitor *erythro*9-(2-hydroxy-3-nonyl)adenine [(+)-EHNA] over a range of concentrations were used to monitor inhibitor effects on F-ddA absorption and metabolism.

Results. High concentrations of EHNA in coperfusions with F-ddA completely inhibited intestinal ADA, increasing the permeability coefficient of F-ddA by nearly threefold but producing high systemic inhibition of ADA. Mathematical models were utilized to show that in full-length intestinal perfusions an optimal log mean lumenal EHNA perfusate concentration of 0.5 μg/ml could achieve an intestinal bioavailability of 80% with <20% systemic inhibition.

Conclusions. Optimizing local enzyme inhibition may require careful selection of a suitable inhibitor, the dose of the inhibitor, and the inhibitor vs. drug absorption profiles.

KEY WORDS: F-ddA; adenosine deaminase; EHNA; intestinal metabolism; bioavailability; intestinal permeability; dideoxynucleosides; HIV; AIDS.

INTRODUCTION

Presystemic intestinal metabolism is an increasingly recognized barrier to the absorption of oral medications. Among the enzymes found in the intestine are cytochrome P450s, proteases, esterases, and various conjugative and nucleoside salvage enzymes (1–3). These enzymes may represent the primary barrier to absorption of certain therapeutic agents.

Oral administration of anti-HIV agents is essential for their commercialization, as they must be taken regularly for many years. However, many agents currently marketed or in development are substrates for intestinal enzymes or efflux transporters (2,4–7). For example, (−)-6-aminocarbovir (6AC) and 6-chloro-2′3′-dideoxypurine (6-Cl-ddP), adenosine deaminase (ADA) activated prodrugs with potential as central nervous system (CNS)-targeted precursors of the active anti-HIV agents (−)-carbovir and 2′,3′-dideoxyinosine (ddI), are degraded extensively by intestinal ADA during absorption (5–7). These prodrugs increase the availability of their parent dideoxynucleosides, but poor oral bioavailability of the intact prodrugs limits their effectiveness in treating AIDS dementia or in eliminating HIV from sanctuary sites in the brain.

Inhibitors of intestinal enzymes or transporters have shown promise in enhancing the delivery of many anti-HIV agents (8–12), but the practical application of these approaches *in vivo* may be difficult. Increasing inhibitor concentrations may increase oral availability, but may also lead to unwanted and potentially prolonged systemic enzyme inhibition. Thus, the selection of an inhibitor is a balancing act. The permeation of the inhibitor must be sufficient to reach the enzyme, but not so high as to result in inhibitor depletion over the length of intestine needed for a substantial fraction of the drug to be absorbed. A single inhibitor may not be the best choice for a wide range of substrates for any given enzyme.

EHNA has been shown to exhibit a suitable permeability profile and potency to enhance the oral bioavailability of 6-Cl-ddP without causing unacceptable levels of systemic inhibition (11,12). To determine the extent to which EHNA may be considered as a universal local inhibitor of ADA, this study explores its utility in enhancing the oral absorption of another ADA activated anti-HIV prodrug, 2′-β-fluoro-2′,3′-dideoxyadenosine (F-ddA). F-ddA, a prodrug of 2′-β-fluoro-2′,3′-dideoxyinosine (F-ddI), was selected for clinical studies as an acid stable prodrug with potentially improved bioavailability and CNS penetration (13). However, in Phase I clinical trials the oral bioavailability of F-ddA was 67 ± 21% in terms of total dideoxynucleoside, but <10% appeared in the systemic circulation as intact prodrug due to intestinal metabolism by ADA (14). F-ddA is less lipophilic and a better ADA substrate than 6-Cl-ddP and therefore represents a greater challenge for the local inhibition approach utilizing EHNA.

MATERIALS AND METHODS

Chemicals

F-ddA, F-ddI, and (+)-EHNA (Fig. 1) were obtained from the National Cancer Institute, National Institutes of Health (Bethesda, MD). 2′,3′-Dideoxyadenosine (ddA) and ddI were provided by the National Institute of Allergy and Infectious Diseases. All other chemicals were of analytical reagent grade.

Animals

Male Sprague-Dawley rats (300–325 g, Simonsen Laboratories, Gilroy, CA) were housed and cared for at the Animal Resource Center, University of Utah, according to the

[1] Division of Pharmaceutical Sciences, College of Pharmacy, University of Kentucky, Lexington, KY 40536.

[2] To whom correspondence should be addressed. (e-mail:bande2@pop.uky.edu)

ABBREVIATIONS: F-ddA, 2-β-fluoro-2′,3′-dideoxyadenosine; F-ddI, 2-β-fluoro-2′,3′-dideoxyinosine; ADA, adenosine deaminase; (+)-EHNA, *erythro*9-(2-hydroxy-3-nonyl)adenine; CNS, central nervous system; DCF, 2′-deoxycoformycin; 6AC, (−)-6-aminocarbovir; <EHNA>, log mean lumenal EHNA concentration.

0724-8741/01/0900-1270$19.50/0

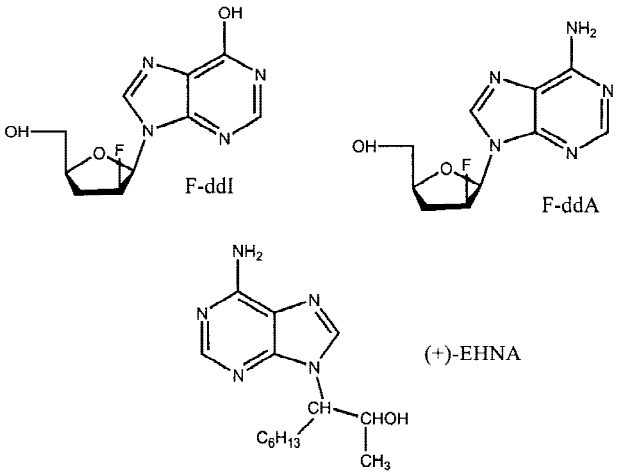

Fig. 1. Structures of F-ddA, F-ddI, and (+)-EHNA.

United States Department of Agriculture Animal Welfare Act and the National Institutes of Health Principles of Laboratory Animal Care.

Intestinal Transport

Perfusion experiments with mesenteric vein cannulation to monitor intestinal uptake and metabolism were described previously (12). Briefly, the animal was placed under halothane anesthesia and the jugular vein was cannulated (silastic tubing). If the animal was used as a blood donor, 1000 units of heparin was administered through the cannula, followed by collection of blood into a vial containing 100 units of heparin. In rats used for intestinal perfusion, jugular vein cannulation was followed by cannulation of a 6–13 cm ileal segment. The mesenteric vein leading from that segment was isolated and cannulated such that all blood leaving the segment was collected. Blood infusion was then initiated through the jugular cannula to replace blood lost. Prior to surgery, F-ddA solutions (~180 μg/ml) with or without EHNA (0.04–100 μg/ml) were prepared in perfusion buffer (8.0 g/L $NaH_2PO_4 \cdot H_2O$ and 11.3 g/L Na_2SO_4, pH 7.4 [NaOH] and 290–310 mOsm [NaCl]). The solutions were filtered (0.45 μm nylon syringe filter) and perfused through the ileum at 1.0 ml/min for the first minute to fill the segment and 0.2 ml/min thereafter. Perfusate and mesenteric blood were collected continuously in preweighed vials, weighed, quenched with 15 ml CH_3CN, and stored at –20°C until analysis by HPLC.

EHNA Systemic Inhibition

Animals for systemic inhibition studies were cannulated at the jugular vein, as described, for systemic blood sampling. A 10 cm ileal segment was cannulated as described with care taken to ensure that the absorption surface area was the same for each experiment and the mesenteric capillary bed was undisturbed. Perfusion buffer with EHNA (0.2 to 35 μg/ml) was then perfused through the segment. Perfusate was collected and stored at –20°C until analysis for EHNA by HPLC. Blood (0.7 ml) was collected from the jugular cannula prior to and at 55 and 60 min after the onset of perfusion, and blood ADA activity was determined at 37°C from initial rates of conversion of ddA to ddI. Reactions were initiated by adding 0.2 ml ddA stock solution (6 mg/ml ddA in perfusion buffer) to 1.8 ml diluted blood (1/4 in 0.9% saline) following which 0.2 ml samples were removed, quenched in 1 ml CH_3CN, and frozen at –20°C until analysis for ddI by HPLC.

Sample Preparation and Analysis

F-ddA, F-ddI, ddI, and EHNA were analyzed by HPLC as described previously (12). Analytes were separated on a Supelcosil LC-18S 5 μm column (4.6 mm i.d. × 25 cm) using 13% MeOH, 20% MeOH, and 35% CH_3CN in phosphate buffer (ionic strength 0.02, pH 3.0) for F-ddI and ddI, F-ddA, and EHNA, respectively, with UV detection at 254 nm. A retention volume of 9 ml was observed for all analytes under these conditions. F-ddA recovery in spiked blood was 98 ± 1% ($n = 3$). Recoveries of ddI and EHNA were reported previously (12).

Data Analysis

During intestinal perfusions, the steady-state fluxes for drug disappearing from the lumen (J_{lumen}) and appearing in mesenteric blood (J_{blood}) were:

$$J_{lumen} = QC(0)\left[1 - \frac{C(l)}{C(0)}\right] \quad (1)$$

$$J_{blood} = \frac{\Delta M_B}{\Delta t} \quad (2)$$

where Q is the flow rate through the intestine (0.2 ml/min), and C(0) and C(l) are the concentrations of permeant entering and leaving the segment of length l and radius r (=0.2 cm). Apparent permeability coefficients were calculated from both lumenal disappearance and blood appearance data using Eqs. 3 and 4 (12,15):

$$P_{lumen} = \frac{Q}{2\pi rl} \ln \frac{C(l)}{C(0)} \quad (3)$$

$$P_{blood} = \frac{(\Delta M_B/\Delta t)}{2\pi rl <C>} \quad (4)$$

<C> is the logarithmic mean lumenal concentration of permeant (= {C(0)–C(l)}/ln[C(0)/C(l)]), and $\Delta M_B/\Delta t$ is the steady-state flux of permeant into blood. These and all other permeability coefficients described have units of centimeters per second.

The apparent permeability coefficients calculated from Eqs. 3 and 4 reflect several contributions including aqueous boundary layers on the lumenal and ablumenal sides of the enterocyte, as well as the membrane barrier itself, which contains paracellular and transcellular pathways. Under normal physiological conditions blood flow is considered fast enough that the blood aqueous boundary layer does not pose a significant barrier to mass transport and is usually ignored (15). Apparent permeability can then be represented by Eq. 5:

$$\frac{1}{P_{lumen}} = \frac{1}{P_{ABL}} + \frac{1}{P_m} \quad (5)$$

The intestinal aqueous boundary layer permeability was determined from the hydrodynamic conditions in the intestine at a flow rate of 0.2 ml/min. However, the *in vivo* flow rate in the rat small intestine is 0.063 ml/min (15). Eq. 6 describes the aqueous boundary layer permeability coefficient at different flow rates:

$$P_{ABL} = kQ^n \quad (6)$$

where k and n (1.28×10^{-3} and 0.44, respectively) have been reported previously (15,16).

The membrane permeability coefficient may contain both paracellular (P_{para}) and transcellular (P_{trans}) contributions ($P_m = P_{para} + P_{trans}$) (15). P_{para} depends on permeant size but not permeant lipophilicity. Because the permeants in these experiments are of similar size, a previously estimated P_{para} of 7.0×10^{-7} cm/sec (12) was assumed. The transcellular permeability coefficient (P_{trans}) depends on permeant lipophilicity as described in Eq. 7 (17):

$$\log P_{trans} = s \log K + c \quad (7)$$

where K is the octanol/water partition coefficient. The slope s is a chemical selectivity parameter. An s close to 1 indicates chemical similarity between the bulk solvent and the barrier region of the membrane, whereas s > 1 indicates a more selective barrier, and s < 1 less selectivity. Combining Eqs. 5, 6, and 7 with the value calculated for P_{para} gives a complete description of the apparent permeability coefficient.

The fraction of absorbed prodrug that appears intact in mesenteric blood, defined as the intestinal bioavailability, can be estimated from P_{blood}/P_{lumen}. If hydrolysis by ADA is the only metabolic pathway for F-ddA during its absorption, intestinal bioavailability can also be calculated from the steady-state fluxes of the prodrug and metabolite into the blood and lumen using Eq. 8:

$$\text{Intestinal Bioavailability} = \frac{P_{blood}}{P_{lumen}} \cong \frac{J_{F\text{-}ddA,blood}}{J_{F\text{-}ddA,blood} + J_{F\text{-}ddI,blood} + J_{F\text{-}ddI,lumen}} \quad (8)$$

The apparent ADA inhibition constant, K_i, was estimated from the perfusion data in 10 cm ileal segments using Eqs. 9 (18) and 10 (19):

$$\frac{P_{blood}}{P_{lumen}} = \frac{1}{\cosh(L\sqrt{k_{met}/D})} \quad (9)$$

$$k_{met} = \frac{V_{max}}{K_m\left[1 + \frac{<EHNA>}{K_i}\right]} \quad (10)$$

The model used to estimate systemic ADA inhibition was described previously (11). Absorption of EHNA was determined with *in situ* intestinal perfusion experiments. This information was used to describe an input function for a two-compartment model describing EHNA pharmacokinetic data from intravenous infusions. The composite model yielded the steady-state plasma EHNA concentration. The steady-state EHNA concentration in blood determines the extent of ADA inhibition, which can be estimated from enzyme kinetic parameters obtained in diluted blood after accounting for dilution. The final model was then compared with systemic inhibition data generated from *in situ* perfusions with systemic blood sampling.

Least squares regression analyses were performed using Scientist software (Micromath, Salt Lake City, UT).

RESULTS AND DISCUSSION

EHNA coperfused at high concentration with 6-Cl-ddP, an ADA-activated prodrug of ddI, completely eliminates its intestinal bioconversion to ddI (12). A logarithmic mean lumenal EHNA concentration (<EHNA>) of 0.1 μg/ml increased the ileal segment bioavailability of 6-Cl-ddP from 45% without inhibitor to 90%, with <10% systemic ADA inhibition (11). These promising results suggested that EHNA could also enhance the oral availability of F-ddA. As shown in Table I, however, F-ddA poses a greater challenge because of its lower permeability coefficient reflecting its decreased lipophilicity, combined with a higher susceptibility to ADA metabolism as reflected in V_{max}/K_m.

The activity of ADA is similar in both human and rat intestinal tissues (20). For this reason, and for surgical convenience, the rat ileum was chosen as the site for *in situ* intestinal absorption studies.

Intestinal Absorption and Metabolism of F-ddA

Figure 2 displays the data from a typical *in situ* intestinal perfusion of F-ddA. The closed symbols and right axis represent the ratio of the concentration at the end of the segment of length l (8.6 cm in this example) divided by the initial concentration, C(l)/C(0), and thus reflect the disappearance of F-ddA from the lumen. The open symbols and left axis describe the appearance of F-ddA in blood and F-ddI in blood and lumen. As shown in Fig. 2, the F-ddA concentration exiting the segment is about 92% of the initial concentration and a significant portion of the F-ddA absorbed appears in the blood or lumen as F-ddI. P_{blood} and P_{lumen} calculated using Eqs. 1 and 2 were $(2.8 \pm 0.7) \times 10^{-6}$ and $(55 \pm 15) \times 10^{-6}$ cm/sec, respectively. The magnitude of the discrepancy in the permeability coefficients indicates a substantial metabolic barrier to F-ddA absorption. From Eq. 8, the intestinal bioavailability, or fraction of absorbed F-ddA that appears in blood intact, was 20 ± 5% with an overall recovery of the F-ddA dose absorbed and subsequently appearing in the blood as F-ddA or in the blood and lumen as F-ddI of 90 × 4% ($n = 7$).

P_{blood} remained constant for perfusate concentrations

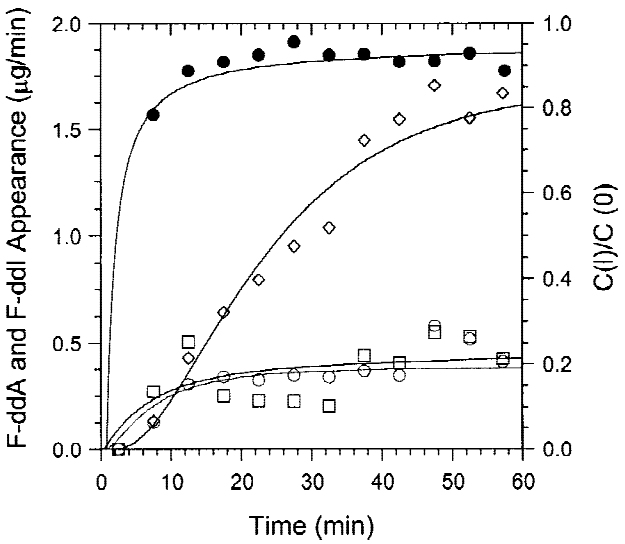

Fig. 2. Representative F-ddA in situ intestinal perfusion data. C(l)/C(0) ratio (●, right axis) and accompanying fluxes of F-ddA in blood (□, left axis), F-ddI in blood (○, left axis), and F-ddI in lumen (◆, left axis).

ranging from 120 to 240 μg/ml (data not shown), a range which exceeds the Michaelis-Menten constant for F-ddA deamination by ADA (K_m = 74 μg/ml). F-ddA incubated at room temperature in perfusate that was passed through the intestine showed <1% degradation in 45 min, indicating that tissue metabolism predominates. The concentration of F-ddA within the enterocyte at steady-state is likely to be below K_m, thus accounting for the apparent linearity in F-ddA availability even at lumenal concentrations exceeding K_m.

Flux of F-ddI back into the intestinal lumen accounts for >50%, a significant portion of the absorbed dose and substantially more than that seen with 6-Cl-ddP, where back-flux of ddI into the lumen accounted for <25% of the total prodrug absorbed. Because F-ddA penetrates the intestinal barrier more slowly than 6-Cl-ddP and is metabolized more rapidly with a V_{max}/K_m nearly tenfold higher than that for 6-Cl-ddP, the site of F-ddA bioconversion is likely to be closer to the lumen giving higher concentrations of F-ddI near the lumenal side of the absorption pathway and thus a higher lumenal back-flux of F-ddI. This argument requires ADA to be present at multiple sites along the absorption pathway, for example, in both the enterocyte and the underlying capillary endothelial cells within the villus microcirculation, or alternatively, drug concentration gradients may develop within the enterocyte if it is not a well-mixed compartment.

Also apparent in Fig. 2, F-ddA and F-ddI blood concentrations reach steady-state within 15 to 20 min after the onset of perfusion, but the lumenal concentration of F-ddI does not appear to reach steady-state within the 60 min perfusion. 6-Cl-ddP perfusions showed a similar slow rise to steady-state for ddI back-flux. Several reasons for this anomaly have been considered, including the hydrodynamics of the system, multiple sites of metabolism, tissue binding, and active transport. The data shown in Fig. 2 were fitted to simplified models containing one and two sites of metabolism. These models used first order kinetic equations to describe the movement of prodrug and metabolite from the lumen to the site(s) of metabolism and into the blood and assumed a logarithmic mean lumenal perfusate concentration in a single well-stirred lumenal compartment. The two-site model gave a longer time to steady-state for F-ddI back-flux and a lower sum of squared deviations. The solid lines in Fig. 2 represent the two-site model. Multiple sites of ADA metabolism along the absorption pathway were previously suggested in studies of the first-pass metabolism of 6-Cl-ddP in the presence of the tight binding but poorly permeable ADA inhibitor 2′-deoxycoformycin (DCF) (11).

Choice of Inhibitor

As shown previously and in Table I, F-ddA undergoes substantially greater ADA-catalyzed bioconversion during its absorption compared to 6-Cl-ddP, so the choice of an inhibitor for F-ddA delivery may be more problematic. There is extensive reference in the literature to the inhibition of ADA (21–25). The two most commonly used ADA inhibitors are EHNA and DCF, and both were examined for their utility as local inhibitors.

Previously, DCF was found to be unsuitable as a local inhibitor for ADA activated prodrugs, as it is too potent, too slowly reversible, and has limited access to at least a portion of the intestinal metabolic sites involved (12). DCF is a much more potent inhibitor than EHNA with a K_I of 0.001 to 0.05 nM, compared with 1 to 20 nM for EHNA. Although DCF shows relatively fast systemic clearance, with a biphasic decline in plasma concentrations with half-lives of 10 and 33 min in normal mice (26), systemic recovery of ADA activity after intraperitoneal DCF administration occurred with a half-life of >10 h (21). Intestinal perfusions of 6AC gave apparent K_I values of 1.2 and 26 μM for EHNA and DCF, respectively, indicating that a much higher lumenal DCF concentration was required to achieve intestinal inhibition compared to EHNA (10).

We previously concluded that EHNA is a preferred candidate for local intestinal ADA inhibition. EHNA shows relatively rapid systemic clearance, exhibiting a biphasic decline in rat plasma concentrations corresponding to half-lives of 2.5 and 18 min (11). Systemic recovery of ADA activity occurred with a half-life of 30 min following intraperitoneal injection (21). Moreover, coperfusions of EHNA with 6AC decreased its gut wall extraction ratio from 54% to <5% (10). Based on this information, EHNA was selected for use in enhancing the delivery of F-ddA.

F-ddA/EHNA Absorption

Figure 3 shows that a coperfusion of F-ddA with a high concentration (47.4 μg/ml) of EHNA in an 8.5 cm ileal segment provides complete intestinal ADA inhibition, evident in the lack of F-ddI appearance in either the blood or lumen.

Table I. Enzyme Kinetic Parameters, Physicochemical Properties, and Apparent Intestinal Permeability Coefficients of Some Dideoxynucleoside Permeants in the Presence and Absence of EHNA

Permeant	V_{max} (μmol/min/unit)	K_m (μM)	V_{max}/K_m (min^{-1}/unit × 10^3)	P_{blood} (cm/sec × 10^6)	P_{lumen} (cm/sec × 10^6)	Partition coeff. (Octanol/water)
ddA	1.1[a]	148[a]	7.4[a]			0.54[b]
	1.32[b]	140[b]	9.4[b]			
		160[d]				
F-ddA	0.23[b]	330[b]	0.70[b]	2.8 ± 0.7 (n = 7)	55 ± 15 (n = 7)	0.66[b]
	0.15[c]	280[c]	0.55[c]			
F-ddI				1.1 ± 0.4 (n = 4)	1.4 ± 0.7 (n = 4)	0.062[b]
F-ddA/EHNA[f]				8 ± 1 (n = 2)	17 ± 7 (n = 2)	
6-Cl-ddP	0.937[c]	12200[c]	0.0768[c]	19 ± 2[d]	84 ± 12[e]	1.7[c]
ddI				1.1 ± 0.3[d]	2 ± 7[d]	0.058[c]
6-Cl-ddP/EHNA[f]				51 ± 7[d]	46 ± 1[d]	

[a] Ref. [11]; [b] Ref. [27]; [c] Ref.[28]; [d] Ref.[29]; [e] Ref.[12]; [f] Perfusate concentration of EHNA >40 μg/ml.

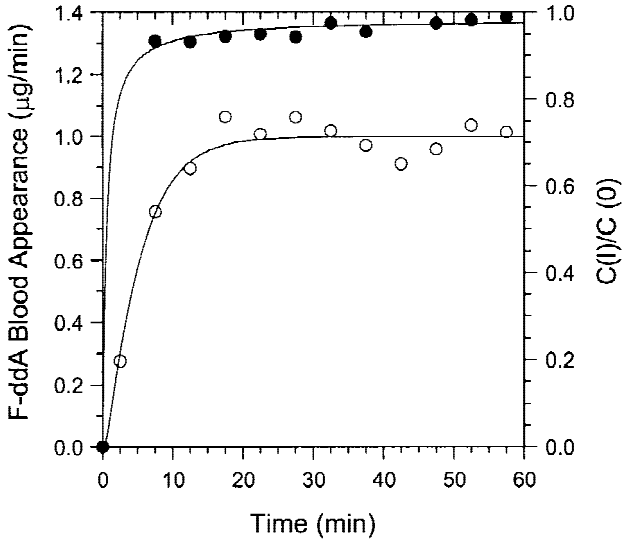

Fig. 3. Representative coperfusion results from F-ddA (245 μg/ml) with EHNA (47.4 μg/ml) in a 10 cm ileal segment. *C(l)/C(0)* ratio (●, right axis) and accompanying F-ddA blood flux (○, left axis) vs. time.

F-ddA concentrations in blood and perfusate reached steady-state within 20 min. With full ADA inhibition, P_{blood} for F-ddA increased nearly threefold to $(8 \pm 1) \times 10^{-6}$ cm/sec, indicating that local inhibition does enhance the intestinal delivery of intact F-ddA. P_{lumen} with full inhibition was much closer to P_{blood} at $(17 \pm 7) \times 10^{-6}$ cm/s. Dideoxynucleoside recovery in blood and perfusate was 97 ± 2%, an increase of 7% from the perfusions of F-ddA in the absence of EHNA. A similar increase was seen in the mass balance in comparing perfusions of 6-Cl-ddP with 6-Cl-ddP/EHNA perfusions.

The apparent permeability coefficients determined with full ADA inhibition represent the best case scenario for enhanced oral delivery with ADA inhibitors. Using Eqs. 5, 6, and 7 the permeability coefficients of several dideoxynucleosides of varying lipophilicity were compared. Figure 4 shows that the permeability coefficients for 6-Cl-ddP and F-ddA with full ADA inhibition correspond to values predicted from their lipophilicity. From the fit, the selectivity parameter s and intercept c from Eq. 7 are 1.7 ± 0.3 and −4.7 ± 0.1, respectively. The intestinal barrier's selectivity appears to differ from octanol, but more experiments will be necessary to verify this.

To further understand the effects of coperfusion of EHNA with F-ddA, and to optimize local inhibition, a range of EHNA concentrations (0.04 to 0.97 μg/ml) were perfused. F-ddA and F-ddI were monitored in blood and perfusate and the extent of intestinal metabolism was determined. The intestinal bioavailabilities determined using Eq. 8 (Fig. 5) indicate that a logarithmic mean lumenal EHNA concentration of 0.5 μg/ml increases the bioavailability of F-ddA from 20% to 80% in a 10 cm ileal segment.

Although EHNA is effective in increasing the systemic delivery of intact F-ddA, it is important to note that the ADA present in mesenteric blood collected from perfusions with high EHNA concentrations was completely inhibited. This may be a cause for concern, because inhibition of systemic ADA should be avoided. However, dilution of the mesenteric blood and a short EHNA pharmacokinetic half-life allow for local inhibition with limited systemic inhibition. In the case of 6-Cl-ddP delivery, an <EHNA> of 0.1 μg/ml was sufficient to

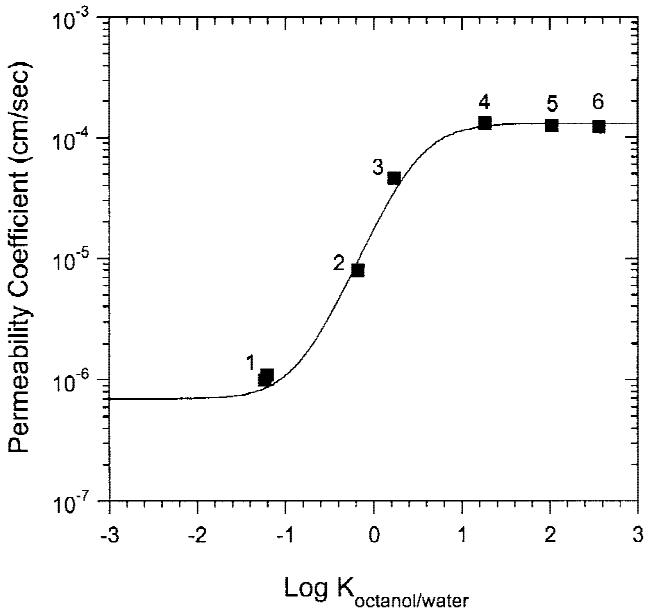

Fig. 4. Apparent permeability coefficients of several dideoxynucleosides vs. log $K_{octanol/water}$ (1 - ddI[12], F-ddI; 2 - F-ddA; 3 - 6-Cl-ddP[12]; 4 - 5′-pivaloyl-6-Cl-ddP[30]; 5 - 5′-(2-ethyl-butyryl)-6-Cl-ddP[30]; 6 - 5′-(2-methyl-benzoyl)-6-Cl-ddP[30]). The solid line represents a fit of Eqs. 5, 6, and 7.

increase intestinal bioavailability to >90% with an estimated systemic ADA inhibition of <10% (12). But the same <EHNA> concentration with F-ddA will only increase its intestinal bioavailability to ~50%. The lower intestinal permeability and higher ADA susceptibility for F-ddA necessitate further optimization.

Systemic ADA Inhibition

Shown in Fig. 6 are experimental values of %ADA inhibition in the systemic circulation resulting from EHNA per-

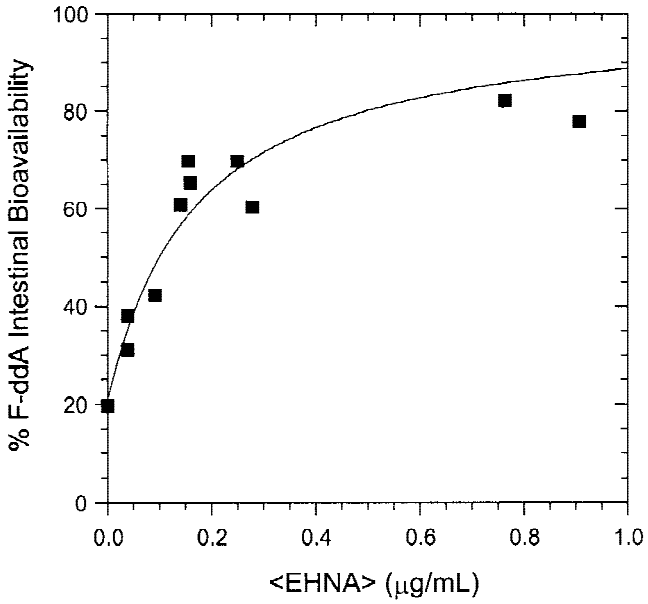

Fig. 5. Intestinal bioavailability of F-ddA vs. logarithmic mean lumenal EHNA perfusate concentrations from *in situ* intestinal perfusion experiments.

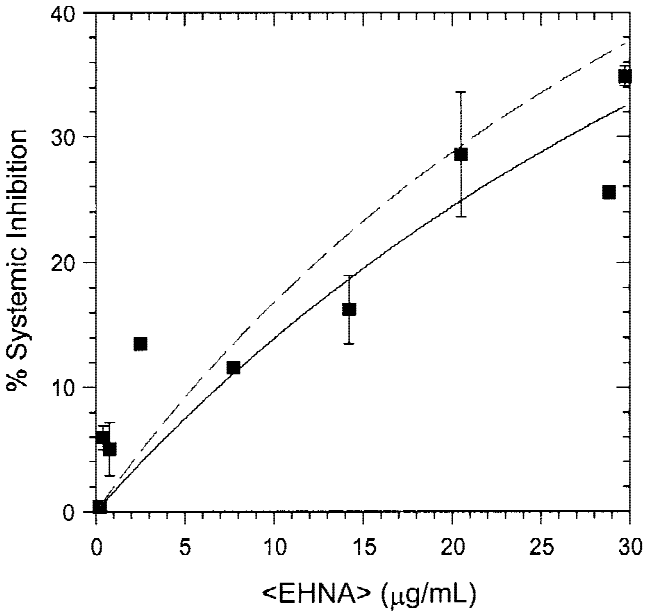

Fig. 6. Systemic blood ADA inhibition measured during EHNA *in situ* intestinal perfusions in 10 cm ileal segments fitted (solid line), or extrapolated (dashed line) based on *in situ* permeability and EHNA pharmacokinetic parameters. Values were measured in 1:4 diluted whole blood.

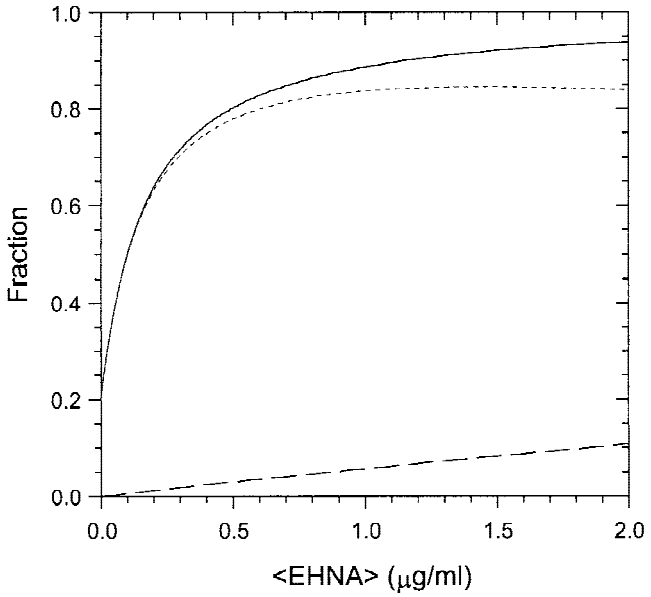

Fig. 7. Intestinal bioavailability of F-ddA (solid line), inhibition of systemic blood ADA (long dashed line), and optimization factors (short dashed line) vs. logarithmic mean lumenal EHNA perfusate concentrations from in situ intestinal perfusion experiments (absorption length = 10 cm).

fusions in a 10 cm ileal segment. The dashed line represents the model predicted value for systemic inhibition from a previous study (11), whereas the solid line represents a least squares fit of the data using the same model employed previously but with either permeability coefficient or K_i being allowed to float while fixing all other parameters. In both cases, the previously determined parameter value, and therefore the extrapolated line previously used, was within the 95% confidence interval of the fitted value indicating that the previous estimate was a good approximation of actual systemic inhibition. All calculations for the optimization of local inhibition in this paper employed the fitted line to describe the extent of systemic inhibition.

Optimizing Local Inhibition

Figure 7 depicts the increasing intestinal bioavailability (solid line) and systemic (blood) ADA inhibition (long dash) with increasing <EHNA>. Intestinal bioavailability approaches a plateau exceeding 90% availability at lumenal inhibitor concentrations, which produce minimal systemic inhibition *in situ*.

Previously, the optimization factor, defined as the product of intestinal bioavailability and the fraction of systemic ADA activity remaining for a given <EHNA>, was utilized to determine the optimal perfusate concentration of EHNA for maximizing intestinal bioavailability while minimizing systemic effects (11). The calculated optimization factor is plotted in Fig. 7 (short dashed line) versus <EHNA> for 10 cm ileal segment perfusions of F-ddA and EHNA. At this absorption length, the curve reaches a plateau value of 0.845 at <EHNA> = 1.45 μg/ml, resulting in <10% systemic inhibition. Local inhibition appears to be quite effective in increasing absorption in a short (10 cm) intestinal segment.

However, the constraints are more severe when the entire length of the intestine (80 to 100 cm in the rat (15)) is considered. Because of their differing absorption profiles, a significant fraction of an F-ddA dose will remain in the lumen after EHNA is depleted below inhibitory levels. At an absorption length of 60 cm the lumenal concentration of F-ddA will be about 33% of its initial value, whereas the EHNA concentration will be <10% of its initial concentration. Depletion of the inhibitor prior to prodrug absorption would result in reduced bioavailability. Future studies will examine and attempt to validate methods for reliably extrapolating these results to the *in vivo* situation.

ACKNOWLEDGMENTS

We thank Dr. Norman F. H. Ho for helpful discussions on intestinal absorption and modeling. This work was supported by an advanced predoctoral fellowship in pharmaceutics from the Pharmaceutical Research and Manufacturers of America Foundation and by a grant from the National Institutes of Health (NS39178).

REFERENCES

1. T. Hasegawa, K. Juni, M. Saneyoshi, and T. Kawaguchi. Intestinal absorption and first-pass elimination of 2′,3′-dideoxynucleosides following oral administration in rats. *Biol. Pharm. Bull.* **19**:599–603 (1996).
2. H. Suzuki and Y. Sugiyama. Role of metabolic enzymes and efflux transporters in the absorption of drugs from the small intestine. *Eur. J. Pharm. Sci.* **12**:3–12 (2000).
3. D. D. Shen, K. L. Kunze, and K. E. Thummel. Enzyme-catalyzed processes of first-pass hepatic and intestinal drug extraction. *Adv. Drug Deliv. Rev.* **27**:99–127 (1997).
4. J. P. Shaw, C. M. Sueoko, R. Oliyai, W. A. Lee, M. N. Arimilli, C. U. Kim, and K. C. Cundy. Metabolism and pharmacokinetics of novel oral prodrugs of 9-[(R)-2- (phosphonomethoxy)propyl] adenine (PMPA) in dogs. *Pharm. Res.* **14**:1824–1829 (1997).
5. C. L. Zimmerman, R. P. Remmel, S. S. Ibrahim, S. A. Beers, and R. Vince. Pharmacokinetic evaluation of (–)-6-aminocarbovir as

a prodrug for (−)- carbovir in rats. *Drug Metab. Dispos.* **20**:47–51 (1992).
6. M. E. Morgan, S.-C. Chi, K. Murakami, H. Mitsuya, and B. D. Anderson. Central nervous system targeting of 2′,3′-dideoxyinosine via adenosine deaminase-activated 6-halo-dideoxypurine prodrugs. *Antimicrob. Agents Chemother.* **36**:2156–2165 (1992).
7. B. D. Anderson, M. E. Morgan, and D. Singhal. Enhanced oral bioavailability of ddI after administration of 6-Cl-ddP, an adenosine deaminase-activated prodrug, to chronically catheterized rats. *Pharm. Res.* **12**:1126–1133 (1995).
8. H. H. Kupferschmidt, K. E. Fattinger, H. R. Ha, F. Follath, and S. Krahenbuhl. Grapefruit juice enhances the bioavailability of the HIV protease inhibitor saquinavir in man. *Br. J. Clin. Pharmacol.* **45**:355–359 (1998).
9. J. Van Gelder, P. Annaert, L. Naesens, E. De Clercq, G. Van den Mooter, R. Kinget, and P. Augustijns. Inhibition of intestinal metabolism of the antiviral ester prodrug bis(POC)-PMPA by nature-identical fruit extracts as a strategy to enhance its oral absorption: An *in vitro* study. *Pharm. Res.* **16**:1035–1040 (1999).
10. C. L. Zimmerman, Y. Wen, and R. P. Remmel. First-pass disposition of (−)-6-aminocarbovir in rats: II. Inhibition of intestinal first-pass metabolism. *Drug Metab. Dispos.* **28**:672–679 (2000).
11. D. Singhal and B. D. Anderson. Optimization of the local inhibition of intestinal adenosine deaminase (ADA) by erythro-9-(2-hydroxy-3-nonyl)adenine: enhanced oral delivery of an ADA-activated prodrug for anti-HIV therapy. *J. Pharm. Sci.* **87**:578–585 (1998).
12. D. Singhal, N. F. Ho, and B. D. Anderson. Absorption and intestinal metabolism of purine dideoxynucleosides and an adenosine deaminase-activated prodrug of 2′,3′-dideoxyinosine in the mesenteric vein cannulated rat ileum. *J. Pharm. Sci.* **87**:569–577 (1998).
13. J. S. Roth, C. M. McCully, F. M. Balis, D. G. Poplack, and J. A. Kelley. 2′-β-Fluoro-2′,3′-dideoxyadenosine, lodenosine, in rhesus monkeys: plasma and cerebrospinal fluid pharmacokinetics and urinary disposition. *Drug Metab. Disp.* **27**:1128–1132 (1999).
14. J. A. Kelley, H. Ford, Jr., J. S. Roth, L. Welles, N. M. Malinowski, R. F. Little, J. A. Leitzau, L. A. Gillim, J. P. Davignon, J. S. Driscoll, and R. Yarchoan. The pharmacokinetics and oral bioavailability of lodenosine (F-ddA), a uniquely stable anti-HIV drug, in adults with sympromatic HIV infection. *Int. Conf. AIDS,* **12**:826 (1998).
15. N. F. Ho, J. Y. Park, P. F. Ni, and W. I. Higuchi. Advancing quantitative and mechanistic approaches in interfacing gastrointestinal drug absorption studies in animals and humans. In W. Crouthamel and A. C. Sarapu (eds.), *Animal Models for Oral Drug Delivery in Man: In Situ and In Vivo Approaches,* APhA, Washington, DC, 1983, pp. 27–106.
16. I. Komiya, J. Y. Park, A. Kamani, N. F. H. Ho, and W. I. Higuchi. Quantitative mechanistic studies in simultaneous fluid flow and intestinal absorption using steroids as model solutes. *Int. J. Pharm.* **4**:249–262 (1980).
17. T.-X. Xiang and B. D. Anderson. Substituent contributions to the transport of substituted p-toluic acids across lipid bilayer membranes. *J. Pharm. Sci.* **83**:1511–1518 (1994).
18. N. F. H. Ho. Biophysical kinetic modeling of buccal absorption. *Adv. Drug Deliv. Rev.* **12**:61–97 (1993).
19. K. F. Tifton. Kinetics and enzyme inhibition studies. In M. Sandler (ed), *Enzyme Inhibitors as Drugs*. University Park, Baltimore, MD 1980, pp. 1–23.
20. D. H. W. Ho, C. Pincus, C. J. Carter, R. S. Benjamin, E. J. Freireich, and G. P. Bodey Sr. Distribution and inhibition of adenosine deaminase in tissues of man, rat, and mouse. *Cancer Treat. Rep.* **64**:629–633 (1980).
21. W. Plunkett, L. Alexander, S. Chubb, and T. L. Loo. Comparison of the activity of 2′-deoxycoformycin and erythro-9-(2-hydroxy-3-nonyl)adenine in vivo. *Biochem. Pharmacol.* **28**:201–206 (1979).
22. R. P. Agarwal, T. Spector, and J. Parks, R. E. Tight binding inhibitors-IV: Inhibition of adenosine deaminase by various inhibitors. *Biochem. Pharmacol.* **26**:359–367 (1977).
23. R. A. Padua, J. D. Geiger, S. M. Delaney, and J. I. Nagy. Rat brain adenosine deaminase after 2′-deoxycoformycin administration: Biochemical properties and evidence for reduced enzyme levels detected by 2′-[^{3}H]deoxycoformycin ligand binding. *J. Neurochem.* **58**:421–429 (1992).
24. W. Plunkett and V. Gandhi. Pharmacology of purine nucleoside analogues. *Hematol. Cell Ther.* **38**:S67–74 (1996).
25. W. D. Klohs and A. J. Kraker. Pentostatin: future directions. *Pharmacol. Rev.* **44**:459–477 (1992).
26. W. R. McConnell, R. L. Furner, and D. L. Hill. Pharmacokinetics of 2′-deoxycoformycin in normal and L1210 leukemic mice. *Drug Metab. Dispos.* **7**:11–13 (1979).
27. J. J. Barchi, Jr., V. E. Marquez, J. S. Driscoll, H. Ford, Jr., H. Mitsuya, T. Shirasaka, S. Aoki, and J. A. Kelley. Potential anti-AIDS drugs. Lipophilic, adenosine deaminase-activated prodrugs. *J. Med. Chem.* **34**:1647–1655 (1991).
28. M. D. Johnson and B. D. Anderson. Localization of purine metabolizing enzymes in bovine brain microvessel endothelial cells: an enzymatic blood-brain barrier for dideoxynucleosides? *Pharm. Res.* **13**:1881–1886 (1996).
29. T. Shirasaka, K. Murakami, H. Ford, J. A. Kelly, H. Yoshioka, E. Kojima, S. Aoki, S. Broder, and H. Mitsuya. Lipophilic halogenated congeners of 2′,3′-dideoxypurine nucleosides active against human immunodeficiency virus in vitro. *Proc. Natl. Acad. Sci. USA* **87**:9426–9430 (1990).
30. D. Singhal. *Enzymatic Barrier to Oral and Central Nervous System Delivery of Anti-HIV Nucleoside Reverse Transcriptase Inhibitors*. Ph.D. dissertation, Department of Pharmaceutics and Pharmaceutical Chemistry, University of Utah, 1996.